Carrier-density effects in many-polaron systems

M Hohenadler,[1] G Hager,[2] G Wellein,[2] and H Fehske[3]

[1]Theory of Condensed Matter, Cavendish Laboratory, University of Cambridge, United Kingdom
[2]Computing Centre, University of Erlangen, Germany
[3]Institute of Physics, Ernst-Moritz-Arndt University Greifswald, Germany

E-mail: mh507@cam.ac.uk

Abstract. Many-polaron systems with finite charge-carrier density are often encountered experimentally. However, until recently, no satisfactory theoretical description of these systems was available even in the framework of simple models such as the one-dimensional spinless Holstein model considered here. In this work, previous results obtained using numerical as well as analytical approaches are reviewed from a unified perspective, focussing on spectral properties which reveal the nature of the quasiparticles in the system. In the adiabatic regime and for intermediate electron-phonon coupling, a carrier-density driven crossover from a polaronic to a rather metallic system takes place. Further insight into the effects due to changes in density is gained by calculating the phonon spectral function, and the fermion-fermion and fermion-lattice correlation functions. Finally, we provide strong evidence against the possibility of phase separation.

PACS numbers: 71.38.-k, 71.27.+a, 63.20.Kr, 63.20.Dj, 71.38.Fp, 71.38.Ht

1. Introduction

The concept of a polaron as a charge carrier bound to a self-created lattice distortion (polarisation) as a result of electron-phonon (EP) interaction has been introduced long ago by Landau [1]. In recent decades, experimental work on a variety of materials has revealed the existence of such quasiparticles in many cases. Of particular interest in this context are colossal-magnetoresistive manganites, in which there is ample experimental evidence for the polaronic character of the charge carriers [2]. More recently, a lot of work on polaron physics has been driven by technological realization of nanostructures such as quantum wells or dots, in which the confinement of carriers usually enhances lattice effects (see [3] and references therein).

Until recently, the bulk of theoretical work on polaronic systems was concerned with the zero-density case (one or two electrons) for which, within the framework of the one-dimensional (1D) Holstein model considered here, it is now well understood that a crossover takes place from a large polaron (extending over more than one lattice site) to a small polaron (with the lattice distortion essentially being localised to the same lattice site as occupied by the electron) upon increasing the EP interaction strength [4, 5] (for a review of spectral properties see [6, 7]). The critical coupling for the crossover sensitively depends on the ratio of the phonon frequency and the electronic hopping integral. Despite a noticeable increase in effective mass in the strong-coupling regime, in a strict sense, polarons remain itinerant quasiparticles at

zero temperature. Quantum phonon fluctuations—not to be neglected in any reliable calculation—strongly affect the transport properties, especially in low-dimensional systems.

Although a detailed understanding of the process of polaron formation in the low-density limit was a necessary first step, real materials are usually characterised by finite charge-carrier densities, so that residual interaction between individual polarons (due to overlap of the phonon clouds) becomes important. For parameters relevant to experiment, a rigorous treatment of density effects [8–12] gives rise to interesting new results [10–12], substantially different from those for a gas of weakly or non-interacting polarons realised, e.g., in the non-adiabatic regime. These discrepancies may also hint at an explanation of the difficulties and inconsistencies arising when fitting experimental data on, e.g., the manganites by using results valid for independent polarons or weak coupling [2, 13].

In this paper, we review and extend recent results on the so-called many-polaron problem in the framework of the 1D spinless Holstein model. To this end, we report on numerical data from exact diagonalisation, cluster perturbation theory and the density-matrix renormalisation group, as well as analytical self-energy calculations, to study photoemission and phonon spectra, optical conductivity as well as static correlation functions. The numerical methods fully take into account quantum phonon effects, and are capable of describing the most important regime of intermediate EP coupling at finite charge-carrier densities.

The paper is organised as follows. The model is introduced in section 2, and a quick overview of the methods employed and a definition of observables is given in section 3. Section 4 is devoted to a discussion of previous and new results on the density dependence of the physics. Finally, we conclude in section 5.

2. Model

As we shall see in section 4, the density dependence of, in particular, the photoemission spectra is quite complicated. Therefore, it is necessary to begin with a simple yet physically reasonable model for a many-polaron system. In this way, the density effects may be understood without additional complications due to, for example, Mott-Hubbard physics occurring in the spinful case [14]. Hence we shall consider the Hamiltonian

$$H = -t \sum_{\langle i,j \rangle} c_i^\dagger c_j + \omega_0 \sum_i b_i^\dagger b_i - g\omega_0 \sum_i \hat{n}_i (b_i^\dagger + b_i)\,. \tag{1}$$

Here $c_i^\dagger$ (c_i) creates (annihilates) a spinless fermion at lattice site i, $b_i^\dagger$ (b_i) creates (annihilates) a phonon at site i, and $\hat{n}_i = c_i^\dagger c_i$. The first term of Hamiltonian (1) describes the hopping of spinless fermions between neighbouring sites $\langle i, j \rangle$ on a 1D lattice. The lattice constant is taken to be unity. The second term accounts for the elastic and kinetic energy of the lattice ($\hbar = 1$) and, finally, the last term constitutes a local coupling of the lattice displacement to the fermion occupation number which can be zero or one.

The model parameters are the hopping integral t, the phonon frequency ω_0, and the coupling constant g. The relation of the atomic-limit polaron binding energy to the latter reads $E_\mathrm{P} = g^2\omega_0$. Introducing the dimensionless quantities $\lambda = E_\mathrm{P}/2t$ and $\gamma = \omega_0/t$ we are left with two independent parameter ratios.

3. Methods

In order to achieve a thorough understanding of the carrier-density dependence of the Holstein model, it is beneficial to make use of both numerical and analytical methods. Whereas large-scale numerical simulations yield exact results for finite systems, approximate analytical calculations yield additional insight into the problem. The methods to be used here have been described in detail elsewhere [10, 15–17].

3.1. Numerical methods

In this paper we use exact diagonalisation (ED) in combination with cluster perturbation theory (CPT) [18, 19] and the kernel polynomial method (KPM) [15], as well as the density-matrix renormalisation group (DMRG) (for adaption of these techniques to coupled EP systems see [16] and references therein). In all cases we employ parallel codes to obtain reliable results for the complex many-body problem under consideration. Furthermore, for most calculations, the homogeneous $q = 0$ lattice distortion has been treated separately to reduce the phonon Hilbert space [20]. All results of this work are for zero temperature. Note that we have in the past also applied a (finite-temperature) quantum Monte Carlo (QMC) algorithm to the present problem [10]. Although the results are consistent with the findings from other approaches, it turns out that the subtle details of the crossover are difficult to see in the calculated single-particle spectra due to temperature effects and the use of the maximum entropy method.

The main observable of interest here is the one-particle spectral function, which provides us with valuable information about the character of the quasiparticles in the system, as well as about the existence of excitation gaps, etc. The transition amplitude for removing ($-$) (adding ($+$)) a free electron—corresponding to (inverse) photoemission—is determined by the imaginary part of the retarded one-particle Green function

$$G^{\pm}(k,\omega) = \lim_{\eta\to 0} \; \langle\psi_0|\, c_k^{\mp} \frac{1}{\omega + \mathrm{i}\eta - H} c_k^{\pm} \,|\psi_0\rangle \;, \tag{2}$$

and hence by the wavevector-resolved spectral function

$$A^{\pm}(k,\omega) = -\frac{1}{\pi}\mathrm{Im}\, G^{\pm}(k,\omega)\,. \tag{3}$$

Here $c_k^{+} = c_k^{\dagger}$, $c_k^{-} = c_k$, and $|\psi_0\rangle$ denotes the ground state of Hamiltonian (1).

The spectral functions (3) can be calculated exactly on small clusters with N lattice sites (and hence for a finite number of wavevectors) with periodic boundary conditions using the KPM. Alternatively, using CPT, we may calculate the real-space cluster Green function $G_{ij}^{c}(\omega)$ of a N_{c}-site cluster with open boundary conditions for all non-equivalent combinations of $i, j = 1, \ldots, N_{\mathrm{c}}$, from which an approximation for the spectrum of the infinite lattice can be obtained by treating the inter-cluster hopping in first-order strong-coupling perturbation theory [18]. Then the partial densities of states (DOSs) are obtained from

$$\rho^{\pm}(\omega) = N_{(\mathrm{c})}^{-1} \sum_{k} A^{\pm}(k,\omega)\,. \tag{4}$$

The phonon spectral function

$$B(q,\omega) = -\frac{1}{\pi}\mathrm{Im}\, D^{\mathrm{R}}(q,\omega) \tag{5}$$

is calculated by using a cluster approximation [6, 7, 21, 22] for the phonon Green function

$$D^{\mathrm{R}}(q,\omega>0)=\lim_{\eta\to 0^+}\langle\psi_0|x_q\frac{1}{\omega+\mathrm{i}\eta-H}x_{-q}|\psi_0\rangle\,, \tag{6}$$

with the phonon coordinates $x_q=N_{\mathrm{c}}^{-1/2}\sum_j x_j e^{-\mathrm{i}qj}$, $x_i=b_i^\dagger+b_i$, and $B(\pm q,\omega)=B(q,\omega)$.

We shall also present KPM results for the linear optical response $\mathrm{Re}\,\sigma(\omega)=\mathcal{D}\delta(\omega)+\sigma^{\mathrm{reg}}(\omega)$ to a longitudinal electric field, with the regular part

$$\sigma^{\mathrm{reg}}(\omega)=\frac{\pi}{N}\sum_{m>0}\frac{|\,\langle\psi_0|\,\hat{\jmath}\,|\psi_m\rangle\,|^2}{E_m-E_0}\,\delta[\omega-(E_m-E_0)]\,. \tag{7}$$

Here E_m is the energy of the m-th eigenstate $|\psi_m\rangle$ of the Hamiltonian (1) defined on an N-site lattice with periodic boundary conditions, and the current operator $\hat{\jmath}=\mathrm{i}\,et\sum_i(c_i^\dagger c_{i+1}-c_{i+1}^\dagger c_i)$.

Finally, we consider the fermion-boson and fermion-fermion correlation functions

$$C_{\mathrm{ep}}(r)=\sum_i\langle(\hat{n}_i-n)x_{i+r}\rangle \tag{8}$$

and

$$C_{\mathrm{ee}}(r)=\sum_i\langle(\hat{n}_i-n)(\hat{n}_{i+r}-n)\rangle\,, \tag{9}$$

respectively. Here $r=0,\ldots,N-1$, and we have introduced the notation $n=N_{\mathrm{e}}/N$ for the carrier density, where N_{e} denotes the number of fermions in the ground state.

3.2. Analytical method

On the analytical side, we shall present recent results from second-order self-energy calculations valid in the weak- and strong-coupling regime, respectively [17]. This approach allows us to calculate the coherent ("c", infinite lifetime) and incoherent ("ic", finite lifetime) contributions to the one-particle (polaron) spectral function given by [17]

$$A_{(\mathrm{p})}(k,\omega)=A^{\mathrm{c}}_{(\mathrm{p})}(k,\omega)\,|_{|\omega|<\omega_0}+A^{\mathrm{ic}}_{(\mathrm{p})}(k,\omega)\,|_{|\omega|\geq\omega_0}\,, \tag{10}$$

where all energies are measured relative to the Fermi energy E_{F}.

4. Results

From previous work [9, 10, 17] (see also references in [17]), the basic effects of variations of the carrier density in the framework of the Hamiltonian (1) are known. It turns out that the physics is particularly simple in the non-adiabatic regime $\gamma\gg 1$, where the quasiparticles are small polarons at all densities at intermediate ($g\simeq 1$) and strong ($g\gg 1$) EP coupling [9, 10, 17]. In contrast, in the experimentally often realised adiabatic regime $\gamma\ll 1$, recent studies have revealed important new effects to be discussed in detail below. Apart from providing a unified discussion of previous work, we present new results to extend the present knowledge about the 1D spinless Holstein model.

We shall begin with the limiting cases of weak and strong EP coupling, respectively, for which the calculated spectral functions are rather simple. Due to

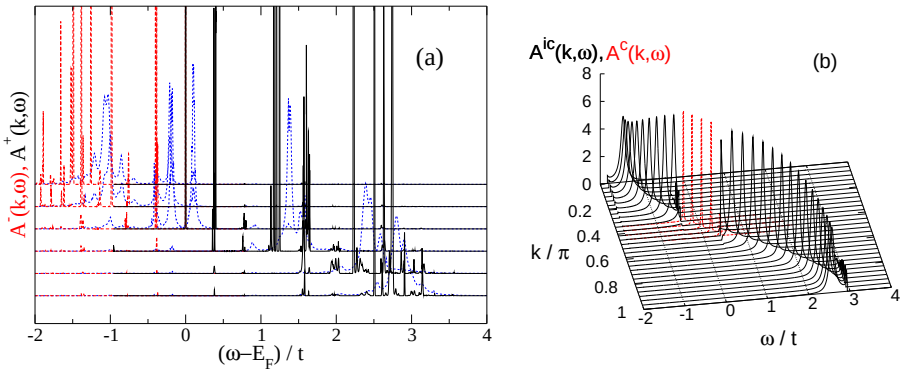

Figure 1. (colour online) (a) Exact diagonalisation results ($N = 10$) for the single-particle spectral functions $A^-(k,\omega)$ (*broken*, red) and $A^+(k,\omega)$ (——, black). Also shown are CPT results for $N_c = 10$ (· · · · · ·, blue). (b) Analytical results for the coherent ($A^c(k,\omega)$, – – –, red) and incoherent ($A^{ic}(k,\omega)$, ——, black) spectral function from the weak-coupling approximation. Here $\gamma = 0.4$, $\lambda = 0.1$, and $n = 0.4$.

the shortcomings of the QMC method used previously, we apply ED and CPT with significantly better energy resolution. Following previous work, we set $\gamma = 0.4$.

The one-electron ground state of the Holstein model is a (weakly-dressed electron) large polaron at (very) weak EP coupling, and a small polaron at strong coupling. For $\gamma < 1$, the crossover between these two regimes takes place at about $\lambda = 1$ [6, 7].

4.1. Weak coupling

For $\lambda \ll 1$, the EP interaction slightly renormalises the charge carriers. Even for large densities n, the spectrum does not change qualitatively [10]. Figure 1(a) shows ED and CPT spectra for $\lambda = 0.1$ and $n = 0.4$. In accordance with QMC calculations [10], the ED results reveal a free-electron like main band (consisting of several discrete peaks on a finite cluster, cf CPT and figure 1(b)) running from -1 to 3 (i.e., having almost the bare bandwidth $4t$). In the vicinity of the Fermi level E_F, the spectrum is dominated by large coherent peaks—small peaks are visible at energies separated from E_F by multiples of ω_0—whereas significant incoherent contributions exist for small or large k. Hence, already for $\lambda = 0.1$, non-trivial effects due to EP coupling are visible.

Figure 1(a) also includes CPT results for $N_c = 10$. However, although reliable results have been obtained with this method in the intermediate coupling regime (see below), CPT fails for the parameters used here. Despite the existence of excitations related to the peaks of the exact results, we find spurious additional peaks having significant spectral weight which are due to the open boundary conditions and the perturbative treatment of the hopping term (see also [21]). For CPT to yield reliable results at weak coupling, even larger clusters would be required to capture the important non-local correlations. Alternatively, the hopping to neighbouring clusters may be treated as a variational parameter [23].

Naturally the small value of λ motivates the use of perturbation theory (in the coupling term). Such calculations, also valid at finite charge-carrier density, have been carried out in [17], and results from the weak-coupling approximation are presented in figure 1(b).

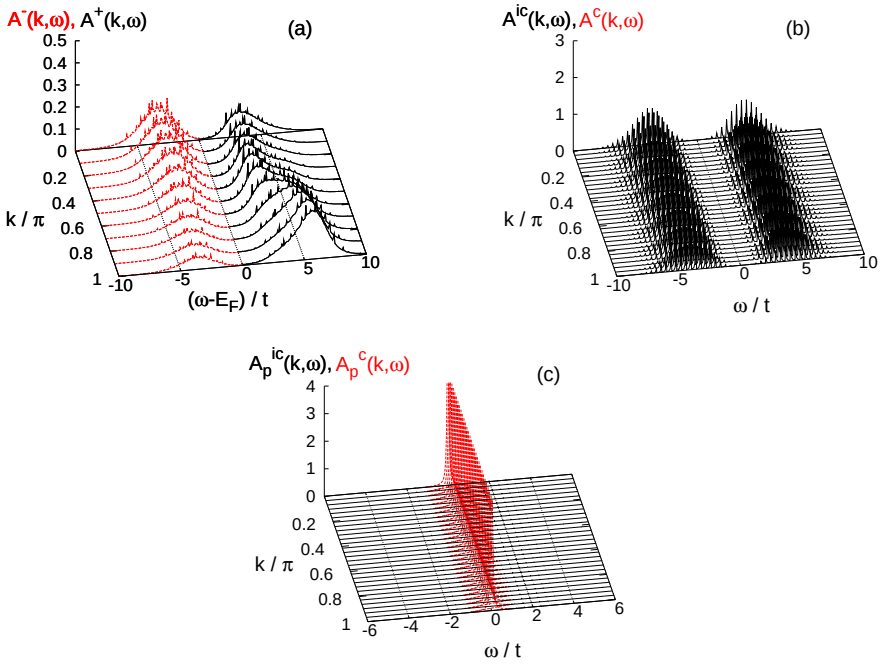

Figure 2. (colour online) As in figure 1, but for strong coupling $\lambda = 2$. CPT results in (a) are for $N_c = 8$ and $n = 0.375$. Analytical results for the electronic spectrum (b) and the polaronic spectrum (c) are from the strong-coupling approximation and for $n = 0.4$. ((b) and (c) taken from [17])

The overall agreement with ED (figure 1(a)) is surprisingly good. The width of the main band fits well that of the numerical spectrum, and even the low-(high-)energy phonon features at small (large) wavevectors are reproduced. Besides, similar to ED, the analytical approach predicts coherent excitations with infinite lifetime for energies $|\omega| < \omega_0$, whereas the CPT spectrum reveals a multi-peak structure and damping even close to E_F.

4.2. Strong coupling

At strong EP coupling, it is well known that the charge carriers are small polarons at low carrier densities, and the spectral properties in this case have been studied intensively (see, e.g., [19, 24, 25]). The density dependence in the many-polaron case has been investigated in [10, 17], suggesting that virtually independent small polarons exist even at large n in the strong-coupling case.

CPT results for $\lambda = 2$ and $n = 0.375$ are shown in figure 2(a) and agree well with previous QMC data [10]. The spectrum is dominated by incoherent (multi-phonon) excitations well below and above the Fermi level, which reveal a Poisson-like distribution and are centred close to $E_P = 4t$. No coherent contributions are visible on the scale of the figure. Despite the higher energy resolution of CPT as compared to QMC, we are not able to monitor the coherent small-polaron band crossing the Fermi level, which gives rise to a finite but small band conductivity. Calculations on

even larger clusters and including more Chebyshev moments are beyond our present computational possibilities.

As in the weak-coupling case, an accurate picture of the physics can be obtained from the analytical approach worked out in [17]. Figure 2(b) shows the electronic spectral function for $n = 0.4$ and the same parameters as in (a). The strong-coupling approximation yields a coherent band with exponentially small spectral weight, and the system may be well characterised as a polaronic metal.

Further evidence for the polaronic nature of the quasiparticles is given by the polaronic spectral function shown in figure 2(c). Here only the coherent small-polaron band with spectral weight $z_k \approx 1$ is visible, and any incoherent peaks—corresponding to electronic contributions—are completely suppressed [17]. Due to the approximations made, the density dependence of the analytical spectra comes out too weak [17] (as compared to QMC [10]).

4.3. Intermediate coupling

It has been stressed above that the intermediate-coupling regime is the most interesting due to the existence of large polarons at low densities, whose overlap gives rise to significant changes with increasing n. We chose $\lambda = 1$, i.e., close to the small-polaron crossover.

Photoemission and phonon spectra Figure 3 shows the photoemission spectra for $n = 0.1$ and 0.3 (left panel), as well as the corresponding phonon spectra (right panel). The results have been obtained by means of CPT and a cluster expansion of the phonon self energy, respectively. Note that in the case of CPT we have not analytically separated the symmetric $q = 0$ phonon mode in calculating $B(q, \omega)$ [15]. This leads to increased numerical effort for the same truncation error.

At low carrier density, figure 3(a), the photoemission spectrum features a polaron band crossing E_F, which flattens at large k where the excitation becomes phononic. Below E_F, we see non-dispersive peaks separated by ω_0 reflecting the Poisson distribution of the phonons in the ground state. Above E_F, incoherent (phonon-mediated electronic) excitations form a broad band with a cosine-like dispersion and a large width of about $4t$. Most importantly, this polaronic spectrum is characterised by a separation between the coherent and incoherent parts of the spectrum, i.e., no low-energy incoherent excitations exist.

The polaronic nature of the spectrum is also reflected in the phonon spectrum $B(q, \omega)$ (figure 3(b)). We see a clear signature of the polaron band at low energies, which fits well the renormalised polaron band dispersion in the thermodynamic limit. At higher energies, close to the bare phonon energy, an almost flat band—overlaid by an excited "mirror polaron band"—is found [22].

Increasing the density to $n = 0.3$ (figure 3(c)), we find that a polaron band can hardly be identified. There is no longer a clear separation between coherent and incoherent parts. Instead, a broad (width $\approx 6t$) main band, formed by the merged phonon peaks below E_F and by incoherent electronic excitations above E_F, crosses the Fermi level. Such a spectrum is reminiscent of the metallic system with carriers renormalised by diffusive phonon scattering.

This qualitative change of the nature of the quasiparticles is also reflected in the phonon spectrum. As shown in the figure 3(d), there is no longer a well-defined polaronic signature in $B(q, \omega)$ (cf figure 3(b)). Instead, we observe at larger q an

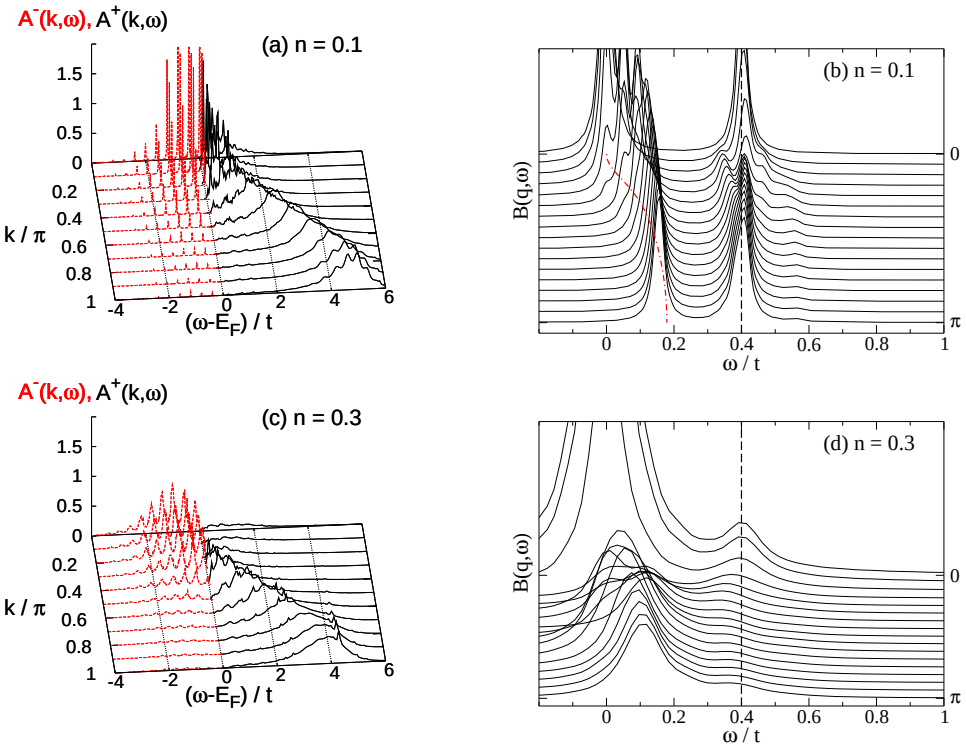

Figure 3. (colour online) (a) and (c): CPT results ($N_c = 10$) for the single-particle spectral functions $A^-(k,\omega)$ (– – –, red) and $A^+(k,\omega)$ (——, black) for $\gamma = 0.4$, intermediate coupling $\lambda = 1.0$ and different densities n. (taken from [11]) (b) and (d): phonon spectral function $B(q,\omega)$ (——) from the cluster expansion ($N_c = 10$) for the same parameters. Also shown are the polaron band dispersion $E(k) - E(0)$ [22] (— · —, red, in (b) only) and the bare phonon frequency (– – –). ((b) taken from [22])

excitation band extending over a broad range of ω values. There is also a strong suppression of the signal at $\omega = \omega_0$, indicating that diffusive scattering dominates.

Optical response The density-driven changes are also visible in the optical response of the system shown in figure 4. For the sake of clarity, we discuss the latter together with results for the DOS which of course reflects the features of the spectral function discussed above (cf equation (4)).

For $n = 0.1$, we notice from the DOS a polaron feature at the Fermi level, characterised by a (moderate) jump in the integrated DOS at E_F and the low spectral weight of $\rho^-(\omega < E_F)$. Owing to the choice $\lambda = 1$, i.e., the existence of a large polaron, the corresponding optical response $\sigma^{reg}(\omega)$ in figure 4(b) strongly deviates from the analytical strong-coupling result [26]. In particular, the maximum in σ^{reg} occurs well below the small-polaron value $2E_P$.

At $n = 0.3$ (figure 4(c) and (d)) the system shows enhanced transport. The polarons are dissociated and the remaining electronic quasiparticles are scattered by virtual phonons. As a consequence, a description of the optical response in terms of

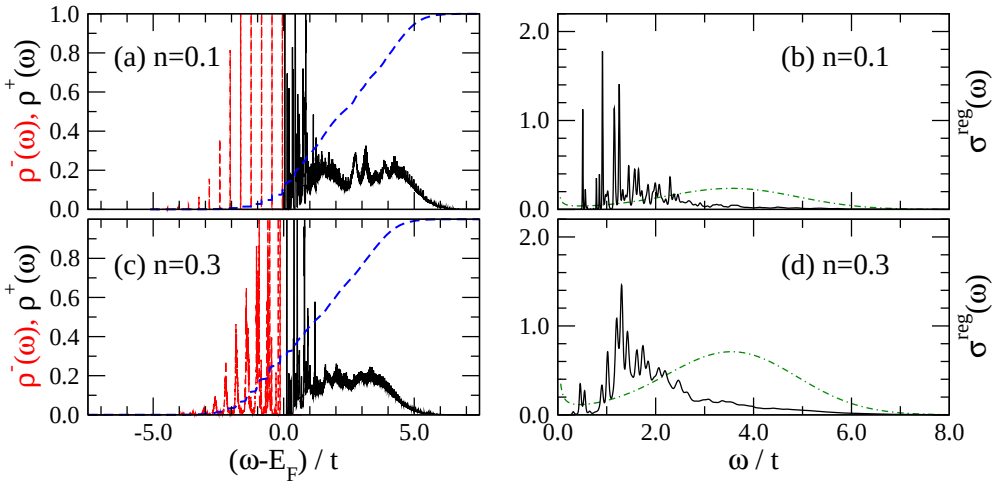

Figure 4. (colour online) (a) and (c): ED results ($N = 10$) for the partial DOSs $\rho^-(\omega)$ (– – –, red) and $\rho^+(\omega)$ (——, black) for $\lambda = 1$, $\gamma = 0.4$ and different band fillings n. (b) and (d): Regular part of the optical conductivity $\sigma^{\rm reg}(\omega)$. Also shown (— · —, green): analytical strong-coupling result $\sigma^{\rm reg}(\omega) = \sigma_0\, n\, (\omega_0 g)^{-1}\, \omega^{-1}\, \exp[(\omega - 2g^2\omega_0)/(2g\omega_0)]^2$ ($\sigma_0 = 8$) [26]. (taken from [12])

small-polaron theory breaks down completely.

The change in the nature of the charge carriers in going from $n = 0.1$ to 0.3 is also reflected in the Drude part $\mathcal{D}$ of the optical response. The one-band sum rule for $\mathrm{Re}\,\sigma(\omega)$ reads $-E_{\rm kin}/2 = \mathcal{D} + \int_0^\infty \mathrm{d}\omega \sigma^{\rm reg}(\omega)$. Whereas for a single electron in the small-polaron regime the kinetic energy is dominated by the regular part $\sigma^{\rm reg}(\omega)$ (i.e., $\mathcal{D} \approx 0$) [27], here we find an increase of the ratio of $\mathcal{D}$ to $\int_0^\infty \mathrm{d}\omega \sigma^{\rm reg}(\omega)$ from 3.9 ($n = 0.1$) to 4.1 ($n = 0.3$). This indicates that transport becomes more coherent at large densities due to polaron dissociation.

Correlation functions The spectral properties calculated so far clearly show the qualitative change in the nature of the ground state with increasing density. Since we expect these changes to result from a dissociation of individual polarons, it is highly desirable to calculate quantities which provide direct proof for this mechanism. Therefore, we study here the correlation functions $C_{\rm ep}(r)$ and $C_{\rm ee}(r)$ (see equations (8) and (9)), which have been defined such as to permit comparison of different n. Accounting for the homogeneous lattice distortion $\langle x \rangle = 2ng$ and the average electron density n, respectively, we have $\sum_r C_{\rm ep}(r) = 0$ and $\sum_r C_{\rm ee}(r) = 0$. Furthermore, the data in figure 5 have been rescaled by the number of electrons $N_{\rm e}$.

Figure 5(a) shows $C_{\rm ep}(r)$ for selected densities n, obtained on a cluster with $N = 24$ using the DMRG. For the observables and parameters considered here, the results are only weakly sensitive to the choice of boundary conditions (periodic or anti-periodic, see caption of figure 5).

For a single electron ($n = 0.04$), $C_{\rm ep}(r)$ reveals the existence of a large polaron with a lattice distortion extending over about five lattice sites. Already at $n = 0.17$, the on-site ($r = 0$) correlations are noticeably reduced, whereas $C_{\rm ep}(r > 0)$ is increased as compared to $n = 0.04$. Increasing the density even further to $n = 0.29$—roughly where a polaron band can no longer be identified in the photoemission spectrum (see

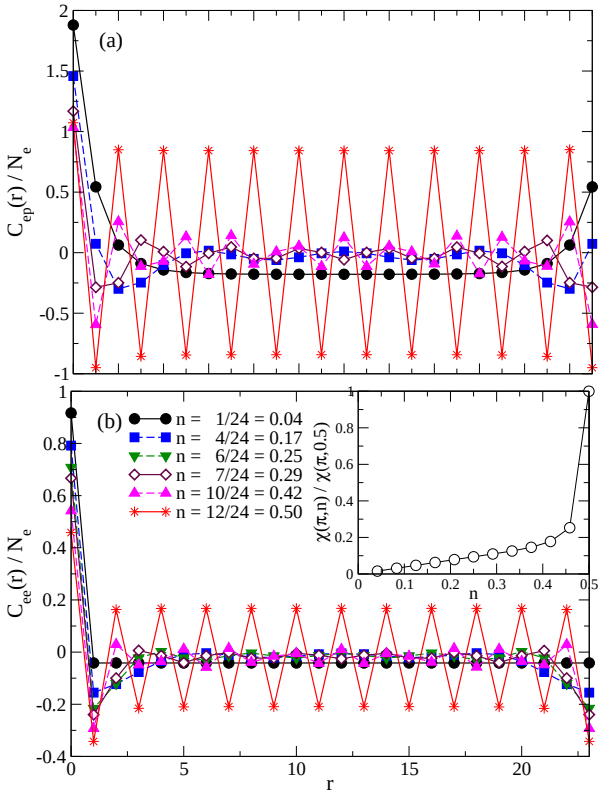

Figure 5. (colour online) DMRG results ($N = 24$) for the correlation functions (a) $C_{\rm ep}(r)$ and (b) $C_{\rm ee}(r)$ (normalised by the number of electrons $N_{\rm e}$) for different band fillings n. The inset in (b) shows the renormalised charge-structure factor $\chi(\pi) = N^{-2}\sum_{ij}(-1)^{i+j}\langle n_i n_j\rangle$. Here, $\gamma = 0.4$ and $\lambda = 1$. Results have been obtained using anti-periodic (periodic) boundary conditions for even (odd) $N_{\rm e}$ (also in figure 6, see [28]).

figure 3(b))—we see a rather homogeneous value $C_{\rm ep}(r) = 0$ (the average distortion has been subtracted) for almost all values of r. This is exactly what we expect for a system of electrons and unbound phonons. $C_{\rm ep}(r)$ starts to fluctuate as we go to even large n since we approach the Peierls transition. At $n = 0.5$, in the thermodynamic limit, the latter leads to long-range charge-density-wave order with alternating occupied and empty lattice sites, causing symmetric fluctuations in $C_{\rm ep}(r)$ [21].

The corresponding results for the fermion-fermion correlation function $C_{\rm ee}(r)$ show a very similar density dependence. An interesting open question concerns the possibility of charge density wave formation in the present model at other commensurate densities such as 1/4 or 1/3. Although the critical EP coupling for the transition to such insulating states is expected to be significantly larger than at half filling, due to reduced Umklapp scattering and the absence of perfect nesting, figure 5 indeed reveals $N_{\rm e}$ maxima for, e.g., $n = 0.25$. In the thermodynamic limit, charge ordering may thus be realised at commensurate fillings away from $n = 0.5$.

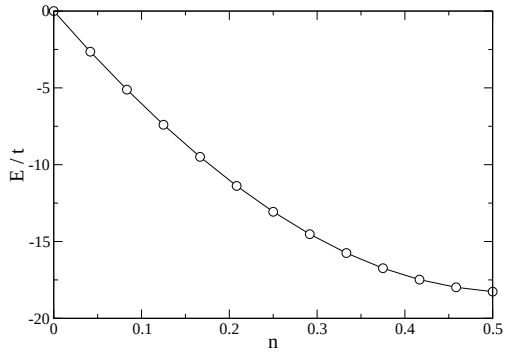

Figure 6. DMRG results for the ground-state energy E as a function of band filling n. Here $N = 24$, $\gamma = 0.4$ and $\lambda = 1$. Lines are guides to the eye.

Absence of phase separation Finally, we consider the possibility of phase separation of polarons. It is known from the spinful Holstein model that real-space pairing of electrons into bipolarons can occur if the EP-mediated attraction overcomes the kinetic and Coulomb energy. Hence, one might expect aggregation of polarons in one region of the system, i.e., a clustering of polarons (polaron droplets) or bipolarons. Phase separation might also appear when doping the system away from the half-filled (charge-ordered) band case.

To approve or rule out this possibility, we calculate the ground-state energy as a function of carrier density using the DMRG. The latter approach permits us to consider a large cluster with $N = 24$—the number of fermions $N_\mathrm{e} = 1 \ldots 12$—so that we can increment n in rather small steps. Any tendency toward phase separation should manifest itself by non-convex behaviour of E as a function of n. The results, presented in figure 6, provide strong evidence for the absence of phase separation in the model considered here. As a consequence of the very small binding energy in the model with two electrons [29], the tendency towards pairing is also suppressed as compared to the spinful case.

5. Conclusions

Using a variety of different and in many aspects complementary methods, we have obtained a rather complete understanding of the many-polaron problem in the framework of the one-dimensional spinless Holstein model. Whereas the physics is simple in the limiting cases of weak or strong electron-phonon interaction, or in the non-adiabatic regime—the charge carriers being either weakly renormalised electrons or small polarons—substantial density effects are observed in the (adiabatic) intermediate-coupling case.

Starting from low densities $n \ll 1$ (the single-polaron problem), the nature of the charge carriers changes from large polarons to renormalised electrons, resulting in a metallic system at intermediate carrier densities $n \approx 0.3$. This crossover has been investigated by studying photoemission spectra, phonon spectra, optical response, fermion-lattice and fermion-fermion correlation functions. All these observables support the hypothesis of dissociation of large polarons in a conclusive way.

Furthermore, by calculating the ground-state energy as a function of n up to

$n = 0.5$, we can strongly argue against phase separation of polarons. Interestingly, the results point toward the occurrence of lattice instabilities accompanied by charge ordering at commensurate fillings other than 0.5, but this issue needs further investigation.

The present work is restricted to a rather simple model. However, the density effects on the nature of the charge carriers arise from the residual interaction (overlap) of extended polarons. Such a basic mechanism may be expected to be important also in more involved models (e.g., with long-range interactions and spin, or in higher dimensions—large polarons exist in Fröhlich models also for $D > 1$).

There is also no reason to expect the absence of similar physics in dense polaronic systems such as the manganites, especially as recent experimental work points towards the existence of large polarons in these materials [13]. The relevance of the effects discussed in this work to realistic materials is further substantiated by the fact that intermediate densities, small but finite phonon frequencies and intermediate couplings are widely regarded as the experimentally most relevant parameter region.

Finally, since existing weak-coupling or low-density theories on the same or similar models do not exhibit the crossover considered here due to the neglect (or insufficient treatment) of density effects, future work on more general many-polaron systems is highly desirable. Despite the greater complexity, it would be important to take into account the spin degrees of freedom, as well as a finite Coulomb repulsion between charge carriers. The rapid increase in computer power opens up the perspective of such studies in the near future.

Acknowledgments

We gratefully acknowledge financial support by the Austrian Science Fund (FWF) through the Erwin-Schrödinger Grant No J2583, the Deutsche Forschungsgemeinschaft through SPP1073, the DFG, KONWIHR, and the European Science Foundation. We would like to thank A Alvermann and J Loos for valuable discussion.

References

[1] L D Landau, Phys. Z. Sowjetunion **3**, 644 (1933).
[2] D M Edwards, Adv. Phys. **51**, 1259 (2002).
[3] M Hohenadler and H Fehske, J. Phys.: Condens. Matter, (2006) editor pls update.
[4] H De Raedt and Ad Lagendijk, Phys. Rev. Lett. **49**, 1522 (1982).
[5] A S Alexandrov and N Mott, *Polarons & Bipolarons* (World Scientific, Singapore, 1995).
[6] H Fehske, A Alvermann, M Hohenadler, and G Wellein, in *Polarons in Bulk Materials and Systems with Reduced Dimensionality, Proc. Int. School of Physics "Enrico Fermi", Course CLXI*, edited by G Iadonisi, J Ranninger, and G De Filippis (IOS Press, Amsterdam, Oxford, Tokio, Washington DC, 2006), pp. 285–296.
[7] H Fehske and S A Trugman, in *Polarons in Advanced Materials*, edited by A S Alexandrov (Canopus Publishing and Springer Verlag GmbH, Bath (UK), 2007).
[8] A S Alexandrov, Phys. Rev. B **46**, 2838 (1992).
[9] M Capone, M Grilli, and W Stephan, Eur. Phys. J. B **11**, 551 (1999).
[10] M Hohenadler, D Neuber, W von der Linden, G Wellein, J Loos, and H Fehske, Phys. Rev. B **71**, 245111 (2005).
[11] M Hohenadler, G Wellein, A Alvermann, and H Fehske, Physica B **378-380**, 64 (2006).
[12] G Wellein, A R Bishop, M Hohenadler, G Schubert, and H Fehske, Physica B **378-380**, 281 (2006).
[13] C Hartinger, F Mayr, J Deisenhofer, A Loidl, and T Kopp, Phys. Rev. B **69**, R100403 (2004).
[14] H Fehske, G Wellein, G Hager, A Weiße, and A R Bishop, Phys. Rev. B **69**, 165115 (2004).
[15] A Weiße, G Wellein, A Alvermann, and H Fehske, Rev. Mod. Phys. **78**, 275 (2006).

[16] E Jeckelmann and H Fehske, in *Polarons in Bulk Materials and Systems with Reduced Dimensionality, Proc. Int. School of Physics "Enrico Fermi", Course CLXI*, edited by G Iadonisi, J Ranninger, and G De Filippis (IOS Press, Amsterdam, Oxford, Tokio, Washington DC, 2006), pp. 247–283.
[17] J Loos, M Hohenadler, and H Fehske, J. Phys.: Condens. Matter **18**, 2453 (2006).
[18] D Sénéchal, D Perez, and M Pioro-Ladrière, Phys. Rev. Lett. **84**, 522 (2000).
[19] M Hohenadler, M Aichhorn, and W von der Linden, Phys. Rev. B **68**, 184304 (2003).
[20] S Sykora, A Hübsch, K W Becker, G Wellein, and H Fehske, Phys. Rev. B **71**, 045112 (2005).
[21] M Hohenadler, G Wellein, A R Bishop, A Alvermann, and H Fehske, Phys. Rev. B **73**, 245120 (2006).
[22] J Loos, M Hohenadler, A Alvermann, and H Fehske, J. Phys.: Condens. Matter **18**, 7299 (2006).
[23] M Potthoff, M Aichhorn, and C Dahnken, Phys. Rev. Lett. **91**, 206402 (2003).
[24] A S Alexandrov, V V Kabanov, and D K Ray, Phys. Rev. B **49**, 9915 (1994).
[25] W Stephan, Phys. Rev. B **54**, 8981 (1996).
[26] D Emin, Phys. Rev. B **48**, 13691 (1993).
[27] J Loos, M Hohenadler, A Alvermann, and H Fehske, (in preparation).
[28] A Weiße and H Fehske, Phys. Rev. B **58**, 13 526 (1998).
[29] M Hohenadler and W von der Linden, in *Polarons in Advanced Materials*, edited by A S Alexandrov (Canopus Publishing and Springer Verlag GmbH, Bath (UK), 2007).